A new ion cyclotron resonance cell for simultaneous trapping of positive and negative ions

Y. Wang and K. P. Wanczek
Institute of Inorganic and Physical Chemistry, Bremen University, Germany

(Received 11 September 1992; accepted for publication 1 December 1992)

In Fourier transform ion cyclotron resonance (ICR) spectrometry until now *either* positive *or* negative ions (including electrons) could be trapped, due to the trapping potential applied. In the present article, the theory of simultaneous trapping of positive and negative ions, and the experimental realization are presented. Trajectory calculations for the ions trapped with both charge polarities are described. The new ICR cell employs a new kind of trapping electrodes, constructed with layers of grids. The simultaneous storage is illustrated by experimentals with sulfur hexafluoride.

I. INTRODUCTION

The fundamental basis for ion cyclotron resonance (ICR) mass spectrometry was established in the early 1930's by E. O. Lawrence.[1] The first practical mass spectrometer based on the cyclotron resonance principle was the omegatron developed in 1949 by Hipple and coworkers,[2,3] and one of the major developments in ICR spectrometry[4] was the introduction of pulsed spectrometry by McIver[5] utilizing a single region trapped ion cell. The main advantage of pulsed operation is the separation in time of ion generation, detection, and quenching. Since Fourier transform (FT) techniques were introduced in the mid-1970's by Comisarow and Marshall,[6,7] FT ICR has been shown to be a powerful tool, of simple mechanical design, capable of accurate mass measurements, with ultrahigh resolution, high upper mass limit, long-time ion storage, and with multichannel advantage, applied to a wide variety of uni- and bimolecular ion reaction. Principles, instrumental developments, and applications of FT ICR spectroscopy has been reviewed.[8–13] However, no matter what applications of FT ICR spectroscopy were developed and what cell structures[14] were used, only ions of one charge sign, positive *or* negative, and only the reactions with neutural molecules could be studied. As is known, ions with both kinds of charges are usually produced during the ionization, desorption, dissociation, and certain ion–molecule reactions processes. Furthermore, the reactions of positive ions (including multi-ionized ions) and negative ion (including electrons), like mutual neutralization and radiative recombination, are natural physical and chemical phenomena, which are of great importance in the study of physical chemistry, astrophysics, atmospheric, and plasma physics.

Although several studies of the ion–ion reactions were undertaken theoretically,[15,16] experimental results are rare. In 1964, Greaves[17] first measured the mutual-neutralization rate coefficients for mass-indentified ions in iodine vapor. In 1968, Aberth *et al.*[18] measured the cross section for mutual neutralization with merging and inclined beam techniques. However, only ion–ion reactions in beams without simultaneous storage and with ions of low masses were studied in their experiments. In addition, in 1971, Schermann and Major[19] investigated the simultaneous storage of Tl^+ and I^- ion in the rf ion trap. However, this kind of ion trap is incapable of trapping positive and negative ions with larger mass difference simultaneously (for example, electrons and ions). Furthermore, it is not possible to detect simultaneously ions with the same mass number but with different charges because of low resolution and of only one charge detection channel in experiments with rf traps.

In this article, principle and design of an ICR cell for simultaneous trapping of positive and negative ions will be described.

There are two methods to trap ions of positive and negative charges simultaneously: An additional ac electric voltage $V\cos\omega t$ is imposed on a pair of trapping electrodes, as shown in Fig. 1(a). The method couples FT ICR with the technique of Paul's rf trap. If the voltage V and frequency ω are properly selected, the ions with both charges and with a certain mass range can be stored in the normal ICR cell. Rempel and Gross[20] have applied this method to increase trapping efficiency during a high pressure event. They employed a relatively high rf amplitude of several hundred volts. The same method[21] has been utilized by Gorshkov, Guan, and Marshall[22] to trap positive and negative ions simultaneously. They employed low ac voltages.

In this article, simultaneous trapping by an appropriate static potential, distributed in the z direction as shown in Fig. 2, is described. To realize the potential, there are several structures of electrodes which can be considered. A preliminary account of this method has been presented.[21] The new ICR cell is shown in Fig. 1(b) and will be described in detail in the experimental section.

II. GENERAL PRINCIPLE

To understand the principle of simultaneous storage, the general ICR principles for singly charged ions are explained with emphasis of the ion storage process. The FT ICR mass spectrometer is based on principles of ion cyclotron resonance. Ions are trapped in an ICR cell by static magnetic (**B**) and electric fields (**E**). Ion motion is governed by the general equation

 0034-6748/93/040883-07$06.00

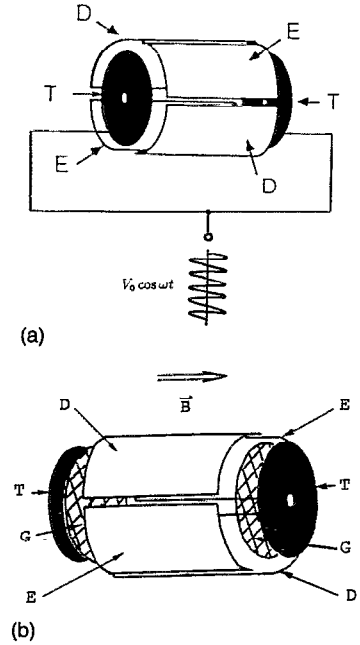

FIG. 1. (a) Simultaneous storage of positive and negative ions in an ICR cell with a Paul's rf technique. T: trapping plates, E: excitation plates, and D: detection plates; (b) with additional grid electodes (G) (details see text).

$$\frac{d\mathbf{v}}{dt}=\frac{q}{m}(\mathbf{E}+\mathbf{v}\times\mathbf{B})-\xi_c\mathbf{v}, \tag{1}$$

where $\mathbf{v}$ is the velocity of the ion, q the ionic charge (C), and m the ionic mass (kg). Collision of the ion with other particles is taken into account through the term ξ_c, the momentum transfer collision frequency, which implies that the average effect of collision is equivalent to a viscous damping term. If the ion experiences only elastic collisions with the neutral species, ξ_c is given by Eq. (2)

$$\xi_c=\frac{nm}{m+M}\langle v_r\sigma_d(v_r)\rangle, \tag{2}$$

where n and M are the number density and mass of the neutral particles, and $\sigma_d(v_r)$ and v_r are the diffusion cross section and the relative velocity of the ion-neutral pair, respectively.[23]

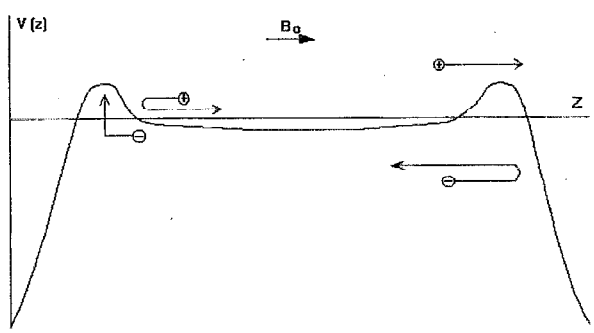

FIG. 2. Static electrical potential for simultaneous storage in the z direction and near z axis. ⊕: positive ions, ⊖: negative ions, and B_0: magnetic field.

In the absence of z motion (along the direction of magnetic field) and of ion collisions, and under the restriction that the electric field is zero everywhere inside the cell, an ion travels along a circular orbit in a plane perpendicular to the magnetic field direction, at the natural cyclotron resonance frequency

$$\omega_c=\frac{qB_0}{m}, \tag{3}$$

where ω_c (rad s^{-1}) is the cyclotron frequency ($2\pi\nu_c$, with ν_c in Hz), B_0 the applied magnetic field strength (T).

According to the evolution of trapped ions three time regimes can be addressed as follows: (i) storage without excitation; (ii) ion excitation; (iii) ion detection. They are described in Secs. II A–II C.

A. Storage without excitation

Ions are produced initially from neutral gas in the cell by electron impact ionization, which initially localizes the ion cloud along the electron beam. In general, the trapping potential near the center of an ICR can be closely approximated by a three-dimensional quadrupolar potential. Therefore, the motion of a single ion in the z direction, the trapping oscillation, is

$$z=\exp\left(-\frac{\xi_c}{2}t\right)\sqrt{z_0^2+\left[\frac{v_z^0+(\xi_c/2)z_0}{\omega_T'}\right]^2}\,\sin(\omega_T't+\phi_p), \tag{4}$$

where

$$\omega_T'=\sqrt{\omega_T^2-\frac{\xi_c^2}{4}}, \tag{5}$$

$$\omega_T=\sqrt{\frac{4S_{T_2}^0qV_T}{mr_0^2}}, \tag{6}$$

and z_0 and v_z^0 are the initial z position and velocity of the ion, ϕ_p is a phase factor, and $S_{T_2}^0$ is a structure constant depending on the specific dimensions of the cell.[24] Normally, ξ_c is small enough compared to ω_T so that ω_T' and ω_T do not differ significantly. Because it is also true in practice that $\xi_c^2 \ll \omega_c^2$ and $\omega_T^2 \ll \omega_c^2$, ion motion in the x and y directions can be closely approximated, in the complex x–y plane, to be

$$r=x+iy=R_{c_0}\exp\left\{-\xi_c\left[1+\frac{\omega_m}{\omega_c}\right]t\right\}\exp[-i(\omega_c-\omega_m)t]$$
$$+R_{m_0}\exp\left(\xi_c\frac{\omega_m}{\omega_c}t\right)\exp(-i\omega_m t), \tag{7}$$

where the first term is the cyclotron motion at effective frequency

$$\omega_{\text{eff}}=\omega_c-\omega_m=\omega_c-\frac{\omega_T^2}{2\omega_c}=\frac{qB_0}{m}-\frac{2S_{T_2}^0V_T}{B_0r_0^2} \tag{8}$$

and the second term is the magnetron motion at frequency

$$\omega_m=\frac{\omega_T^2}{2\omega_c}=\frac{2S^0_{T_2}V_T}{B_0 r_0^2} \tag{9}$$

and R_{c_0} and R_{m_0} are the cyclotron and magnetron radii, respectively.[25] In conclusion, the single ion motion is the superposition of a simple harmonic motion in the z direction at ω_T' with a damped oscillation amplitude, a slow drift of the ion's guiding center about the z axis at ω_m with a magnetron radius which gradually increases when the distance of the guiding center from the center of the cell becomes larger, and the cyclotron motion about the guiding center at ω_{eff} with a gradually decreasing cyclotron radius.

Considering the ion loss by electric field inhomogeneities which results in the steady increase of magnetron radius till the ions are neutralized on the side plates, and taking into account the ion loss due to random walk, the ion trapping efficiency can be characterized by Eq. (10). $t_{1/2}$ is the time needed to decrease the ion concentration to one-half of its initial value

$$t_{1/2}=1.57\times 10^{-28}\frac{(r_0B_0)^2}{P(V_T+0.81)(\alpha\mu_m)^{1/2}}, \tag{10}$$

where P is the pressure (Torr), μ_m the reduced mass (g) for the ion/molecule collision, and α the polarizability of the neutral gas (cm^3).[26] Equation (10) predicts that the ions are trapped more efficiently as the pressure and the trapping voltages decrease and the magnetic field increases.

If the contribution of ionic space charge is included, the dominant effects in the thermalization of the ion cloud are determined by the relative densities of ions and neutral species. If the density of neutral gas is sufficiently high, collisions of ions with neutral species dominate the thermalization process and the ions approach a Maxwell–Boltzmann velocity distribution at about the same rate as they are cooled. Under this condition, ion/neutral reactions are dominant. Alternatively, for sufficiently low neutral densities, the ion–ion self-equilibration rapidly establishes a Boltzmann distribution of ion energies involving a temperature which may be significantly different from the background neutral temperature.[27] The ions in the high energy tail of this distribution with energies greater than the trapping potential energy "evaporate" along the z axis. The corresponding energy inequality can be deduced from Eq. (4)

$$\sqrt{z_0^2+\frac{(V_z^0)^2}{\omega_T^2}}>\frac{a}{2}\quad(t\sim 0,\ \xi_c\ll 1), \tag{11}$$

$$\frac{1}{2}m(V_z^0)^2+2qV_TS^0_{T_2}\frac{z_0^2}{a^2}>qV_T\frac{S^0_{T_2}}{2}, \tag{12}$$

which states that an ion will be lost if its initial (kinetic plus potential) energy of motion in the z direction exceeds the trapping potential energy. This process cools the ion cloud to less than 15% of the well depth ($qV_T/2$) in less than 25 s. After ion–ion self-equilibration, the ion cloud will interact with the neutral gas, as described above, to establish an equilibrium state. Cooling of the ions to thermal equilibrium in the instrument occurs at the ion/neutral collision rate ($\sim$1 s at 10^{-3} mbar). The principal effect of ion space charge is to produce additional electrical fields in radial and in z direction. With the assumption of uniform density of the ion cloud, this effect can be characterized by substituting $S^{0'}_{T_2 z}$ for $S^0_{T_2}$ in Eq. (6) and $S^{0'}_{T_2 r}$ for $S^0_{T_2}$ in Eqs. (8) and (9), where

$$S^{0'}_{T_2 z}=S^0_{T_2}-\frac{q\rho G_{iz}r_0^2}{4\epsilon_0V_T}, \tag{13}$$

$$S^{0'}_{T_2 r}=S^0_{T_2}+\frac{q\rho G_i r_0^2}{4\epsilon_0V_T}, \tag{14}$$

with G_i and G_{iz} are geometric factors of the ion cloud, ρ the ion number density, both of which evolve with time. The time evolution of the ion cloud is that the shape goes from an initially extremely prolate spheroid (infinitely long rod) oriented along the magnetic field to extremely oblate spheroid (infinitesimally thin disk).

B. Ion excitation

Since ions initially have random cyclotron phases (i.e., they are distributed at random initial angles about the z axis), the ion cyclotron motion itself (before excitation) cannot produce a detectable signal. In order to induce a net differential charge between two opposed detector electrodes, the ions must be driven to move coherently, i.e., ions of the same m/q must acquire a nonrandom cyclotron orbital phase. The coherent motion of ions is generated by a rf electric field (orthogonal to $\mathbf{B}_0$) usually produced by applying an rf voltage between two "transmitter" electrodes. If the rf electric excitation field $[E=E_0\exp(-i\omega_c t)]$, circularly polarized with a single frequency for resonance excitation of ions with one m/q ratio, is considered to be spatially uniform and the trapping potential is ignored, the ion trajectories during resonance can be found[28]

$$r=\frac{E_0}{B_0\omega_c}[\exp(-i\omega_c t)-1]+\frac{iE_0 t}{B_0}\exp(-i\omega_c t)+r_0\exp(-i\omega_c t), \tag{15}$$

where complex $r=x+iy$. The term $r_0\exp(-i\omega_c t)$ is related to ion initial position. It can be shown that the ion radius increases linearly with time as the ion speeds up and that the corresponding term is not related to initial conditions. The orbital radius of excited ions is independent of m/q. All ions "lose" the initial phases and are excited to coherent motion. The ions of a given m/q range can be excited to the same ICR orbital radius. The ions with different m/q are excited by multiple frequencies.

C. Ion detection

In FT ICR, the signal is derived from the image current induced by coherent ion cyclotron orbital motion after excitation.[29] A circular cyclotron orbit of an ion after excitation by an electric field for a time T is

$$r_c=(E_0/B_0\omega_c)[\exp(-i\omega_c T)-1]+[(iE_0T/B_0)\times\exp(-i\omega_c T)+r_0\exp(-i\omega_c T)]\exp(-i\omega_c\tau) \tag{16}$$

in which τ is the time after excitation. The superposition of the component image currents of the two receiver plates is amplified, digitized, and stored in the computer for discrete Fourier transformation. This simultaneous observation of all ion species gives the multichannel advantage. The ion number density and the masses of the ions can be obtained by the interpolation procedures described by Serreqi and Comisarow.[30]

III. THEORY

A. Theoretical analysis

In normal ICR cells, both positive and negative ions are confined in x and y directions by the radial force

$$F_r=-|q|B_0\omega r\pm|q|E_0 r \tag{17}$$

in which a strong uniform magnetic field is of main importance and the corresponding term is greater than the term with the electric field. However, in z direction, only ions with one charge sign can be confined by a pair of trapping electrodes, which carry positive voltage for positive ions and negative voltage for negative ions.

Using the method of static electrical potential (refer to Sec. I) and neglecting ion collisions, the equation of motion of positive and negative ions is

$$m^{\pm}\frac{d\mathbf{v}^{\pm}}{dt}=\pm q\mathbf{E}^{\pm}\pm q\mathbf{v}^{\pm}\times\mathbf{B}, \tag{18}$$

where + symbolizes the positive and − the negative ions. For electric field $\mathbf{E}^{\pm}$ the quadrupolar approximation is still used. The equation is expressed in (x,y,z) coordinates as

$$\frac{d^2x^{\pm}}{dt^2}\mp\omega_c^{\pm}\frac{dy^{\pm}}{dt}\mp\frac{2G^{\pm}q}{m^{\pm}}V_{\text{eff}}^{\pm}x^{\pm}=0, \tag{19}$$

$$\frac{d^2y^{\pm}}{dt^2}\pm\omega_c^{\pm}\frac{dx^{\pm}}{dt}\mp\frac{2G^{\pm}q}{m^{\pm}}V_{\text{eff}}^{\pm}y^{\pm}=0,$$

$$\frac{d^2z^{\pm}}{dt^2}\pm\frac{4G^{\pm}q}{m^{\pm}}V_{\text{eff}}^{\pm}z^{\pm}=0, \tag{20}$$

where $\omega_c^{\pm}=(qB_0)/m^{\pm}$, V_{eff} is the effective voltage, and factor G is described in Sec. II. If we combine x and y to a complex r,

$$r=x+iy. \tag{21}$$

Equation (19) can be expressed as

$$\frac{d^2r^{\pm}}{dt^2}\pm i\omega_c^{\pm}\frac{dr^{\pm}}{dt}\mp\frac{2G^{\pm}q}{m^{\pm}}V_{\text{eff}}^{\pm}r^{\pm}=0. \tag{22}$$

We obtain the equation for the eigenvalues $\lambda^{\pm}$,

$$(\lambda^{\pm})^2\pm i\omega_c^{\pm}\lambda^{\pm}\mp\frac{2G^{\pm}q}{m^{\pm}}V_{\text{eff}}^{\pm}=0. \tag{23}$$

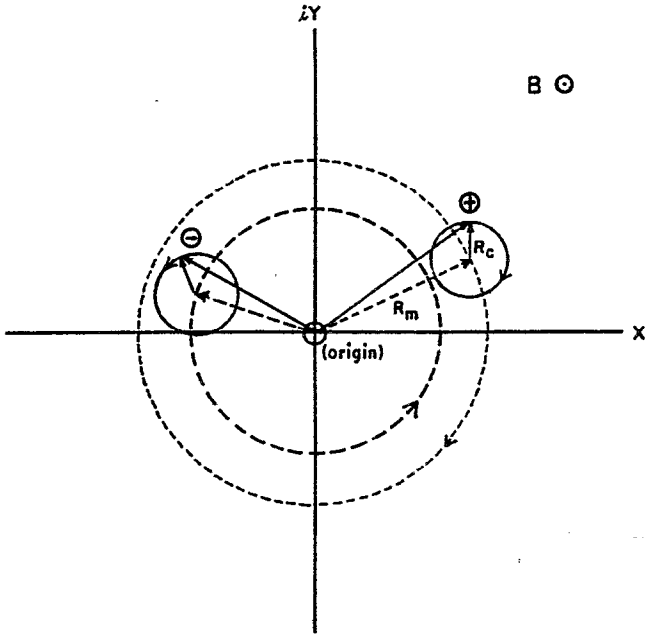

FIG. 3. The motion of ions with different charges in xy cross section in the cell. ⊕: positive ions and ⊖: negative ions. R_0 and R_m are cyclotron and magnetron radii, respectively.

From this equation, the effective motion frequencies of ions with both charges are deduced for positive ions

$$\omega_c'^{+}=\frac{\omega_c^{+}+\sqrt{(\omega_c^{+})^2-4(2G^{+}q/m^{+})V_{\text{eff}}^{+}}}{2}$$

$$\approx\omega_c^{+}-\frac{2G^{+}q}{m^{+}}V_{\text{eff}}^{+},$$

$$\omega_m'^{+}=\frac{\omega_c^{+}-\sqrt{(\omega_c^{+})^2-4(2G^{+}q/m^{+})V_{\text{eff}}^{+}}}{2}\approx\frac{2G^{+}q}{m^{+}}V_{\text{eff}}^{+}, \tag{24}$$

and for negative ions

$$\omega_c'^{-}=\frac{\omega_c^{-}+\sqrt{(\omega_c^{-})^2+4(2G^{-}q/m^{-})V_{\text{eff}}^{-}}}{2}$$

$$\approx\omega_c^{-}+\frac{2G^{-}q}{m^{-}}V_{\text{eff}}^{-},$$

$$\omega_m'^{-}=\frac{\omega_c^{-}-\sqrt{(\omega_c^{-})^2+4(2G^{-}q/m^{-})V_{\text{eff}}^{-}}}{2}$$

$$\approx-\frac{2G^{-}q}{m^{-}}V_{\text{eff}}^{-}, \tag{25}$$

where ω_c' means the effective cyclotron frequency and ω_m' the effective magnetron frequency as indicated in Sec. II. Figure 3 shows the motion of ions with different charges in xy cross section separately: Ions with opposite charges show the same movements which is a superposition of the cyclotron and magnetron motions, however, the direction of rotation is reversed. For positive ions, the effective cyclotron frequency is a little lower than ω_c^{+}, and for negative ions a little higher than ω_c^{-} if $V_{\text{eff}}^{\pm}$ are positive.

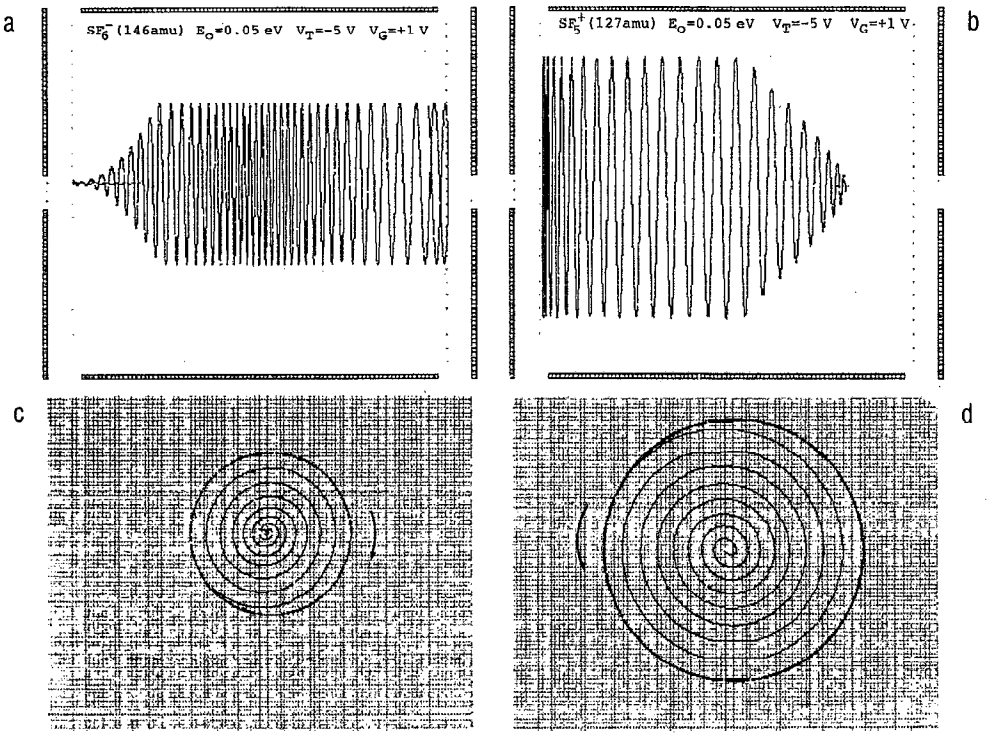

FIG. 4. Simulated motion of positive SF_5^+ ions [(b) and (d)] and negative SF_6^- ions [(a) and (c)] in z [(a) and (b)] and r [(c) and (d)] directions.

B. Simulation

The above theoretical analysis is qualitative because the approximations described above are introduced. The quantitative analysis of ion motion in three-dimensional space is difficult because of the grid electrodes. To calculate the trajectories of the ions with the SIMION program,[31] nonrotational structure of the grid electrodes have to be simplified to a structure with rotational symmetry. The grids are replaced by sets of concentric rings for the calculation. The computations with sample ions SF_6^- and SF_5^+ reveal that it is possible to store both positive and negative ions in the new ICR cell. The results are shown in Fig. 4. The ion movement in the r direction is as described above.

IV. EXPERIMENT

A. The new ICR cell

The experiments are performed with a prototype Spectrospin FT ICR spectrometer CMS 47. It is equipped with a superconducting magnet of 7.02 T field strength and controlled by an Aspect 3000 computer.

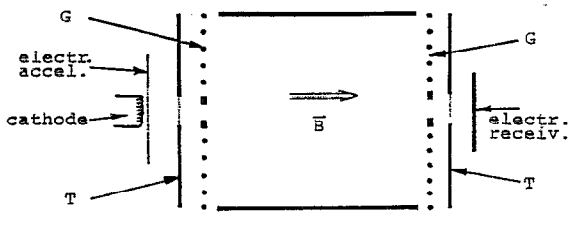

FIG. 5. The cross-sectional diagram of the new ICR cell.

The layout of the new cell is shown in Figs. 1(b) and 5. The cylindrical ICR cell is 42 mm long and has a diameter of 42 mm. The grid electrode (G) in front of the trapping electrods (T) is constructed from mesh with a grid constant of 2 mm. The central hole has a diameter of 4 mm. The distance between the grid and the trapping plate is 1.5 mm.

The base pressure is in the 10^{-10} mbar range and the working pressure of the gas samples is in the 4×10^{-9} mbar range.

The event sequence of experiments is shown in Fig. 6. To quench all charged particles in cell, a series of quench pulses is produced, which consists of an internal quench pulse on the grids (G), an external quench pulse on the trapping electrode (T), and a quench pulse on the side plates (E) [refer to Figs. 1(b) and 5]. In this way the residual positive and negative ions and electrons are elim-

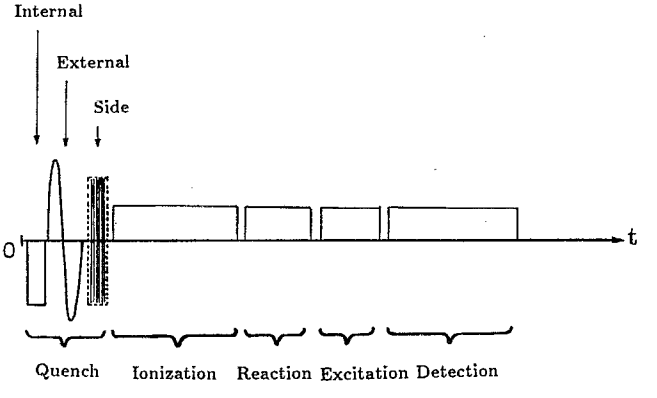

FIG. 6. The time sequence of the experiments.

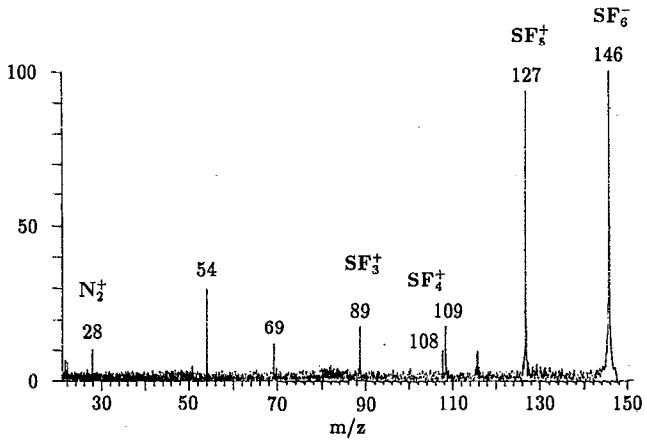

FIG. 7. Mass spectrum with simultaneous storage shows ions SF_6^- (mass number $m/z=146$), SF_5^+ ($m/z=127$), SF_4^+ ($m/z=108$), SF_3^+ ($m/z=89$), and N_2^+ ($m/z=28$). $V_T=-14$ V, $V_G=+0.5$ V.

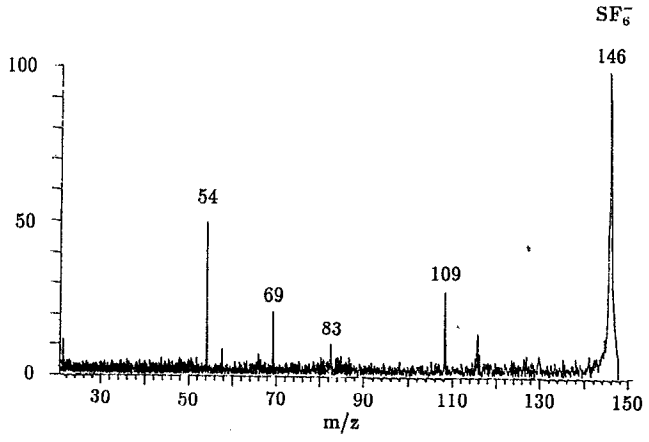

FIG. 9. Mass spectrum of negative ion only: SF_6^- ($m/z=146$). $V_T=-14$ V, $V_G=0$ V.

inated. Ionization of a gas sample by electron impact with electron energy of 70 eV produces ions with both charge polarities. Exitation and detection of the ions of both charges can be performed either simultaneously or after ejection of one kind of ion with the standard detection scheme.

B. Results and discussion

The new method is applied to the ion chemistry of sulfur hexafluoride SF_6. Electron impact ionization of this compound yields the major positive ions SF_5^+, SF_4^+, and SF_3^+. No positive molecular ion SF_6^+ is formed. With the near-thermal electrons, which are formed in large amounts in the ICR cell, the negative molecular ion, SF_6^-, is generated, and with electrons of higher energy, also SF_5^- is formed. In the mass spectrum shown in Fig. 7, all the ions are detected. This indicates the simultaneous storage. The grid voltage can also be adjusted to operate the ICR cell in the "normal" mode to trap only one charge of ion. A positive voltage applied to the grid electrodes and with the trapping electrodes on zero voltage, the mass spectrum shows only positive ions (refer to Fig. 8). In Fig. 9, on the other hand, with the trapping electrodes on negative voltage and the grids on zero voltage, the mass spectrum shows only negative ions. Keeping the voltage of the trapping plates constant, a range of grid voltages exists where both positive and negative ions are trapped. The experiments also show that the relative abundances of SF_5^+ and SF_6^- depend on the voltages of the grid and trapping plates, as shown in Fig. 10. It is clear that there is a common voltage region for simultaneous storage.

The ion motion in the z direction may be analyzed for positive and negative ions separately. We assume that a positive voltage is applied to the grid electrodes and a negative voltage to the trapping plates. For positive ions, the potential distribution in the z direction is shown in Fig. 11(a). As described in Sec. II, the positive ions with energies higher than the maximum energy values of the trapping potential between the grid electrodes will be neutralized on the negative trapping plates. Alternatively, the positive ions with lower energy will be stored in the cell

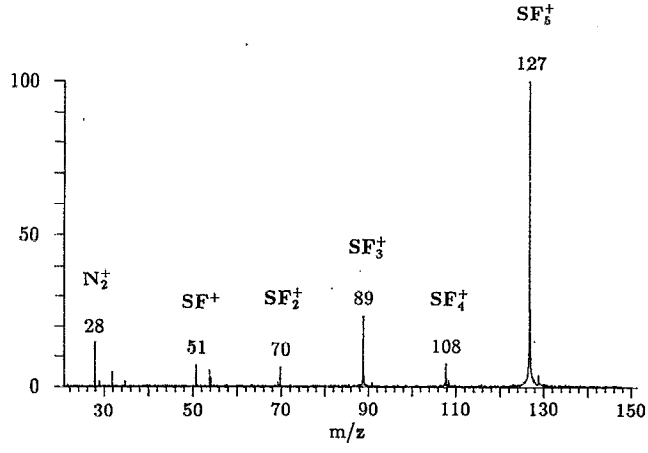

FIG. 8. Mass spectrum of positive ions only: SF_5^+ (mass number $m/z=127$), SF_4^+ ($m/z=108$), SF_3^+ ($m/z=89$), SF_2^+ ($m/z=70$), and N_2^+ ($m/z=28$). $V_T=0$ V; $V_G=+0.5$ V.

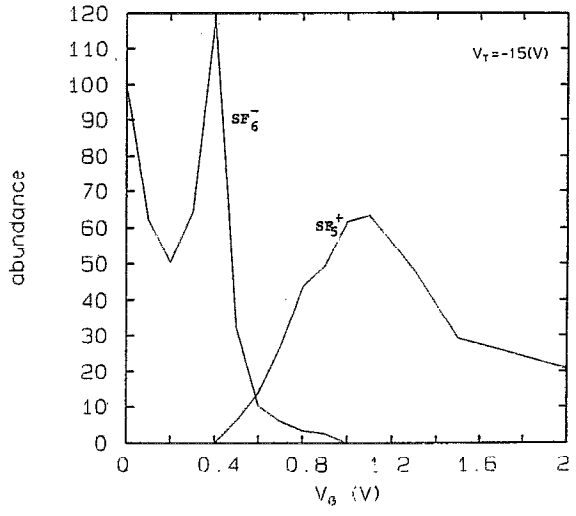

FIG. 10. Relationship between the relative abundances of SF_5^+ and SF_6^- and the grid voltage V_G for a trapping voltage of $V_T=-15$ V.

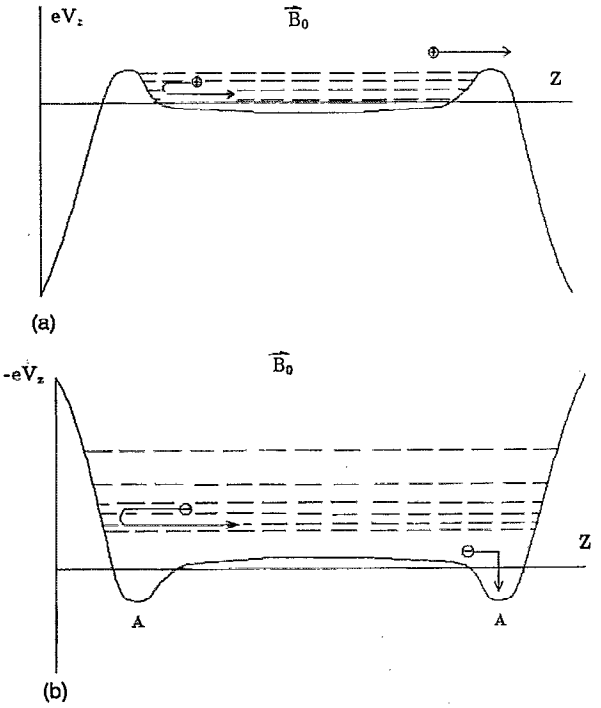

FIG. 11. Potential energy distribution for positive ions (a) and for negative ions (b).

and gradually move to the central region of the cell due to the ion–neutral collisions.

For negative ions, the potential distribution in the z direction is shown in Fig. 11(b). The negative ions with energies higher than the absolute value of the minimum energy for the grid voltage [in Fig. 11(b), the value at point A] will be stored. Because of the big dimension of the mesh, ions will not be lost quickly on the grid electrodes. On the other hand, the negative ions with lower energy will eventually be lost on the grid electrodes during several oscillations around the grids. In order to store the ions of both charges efficiently, the adjustment of the voltages on the electrodes, the dimensions of the mesh, and the distance between grid and trapping electrodes are important factors. These factors influence the trapping efficiency of the positive and negative ions simultaneously. To improve the trapping efficiency for negative ions, there is a small hole in the center of each grid electrode. This improvement does not change the type of the potential distribution described above, but negative ion loss on the grid electrodes is greatly reduced. With the described experimental setup trapping times before excitation are not significantly lower than the trapping times reached for particles of only one charge polarity. However, after excitation, trapping times of positive ions are longer than that of negative ions because negative ions are lost on the grids.

As described above, the positive voltage is applied to the grid electrodes and the negative voltage to the trapping plates, and the negative voltage is greater than the positive voltage. In this way, more electrons can be trapped in the ICR cell, which more efficiently produce the negative ions SF_6^-. If the negative voltage is applied to the grid electrodes and the positive voltage to the trapping plates, the results are vice versa according to charge polarity. However, the less storage of electrons results in the less production of negative ions SF_6^-.

ACKNOWLEDGMENTS

We gratefully acknowledge Pezsa for his technical assistance, and K. H. Kaiser (EMG Co., Bremen) and the development group in Bruker–Franzen Analytik GmbH (Bremen) for mechanical assistance. Also, we thank M. Paul (Bremen University) for his friendly help.

[1] E. O. Lawrence and M. S. Livingston, Phys. Rev. **40**, 19 (1932).
[2] J. A. Hipple, H. Sommer, and H. A. Thomas, Phys. Rev. **76**, 1877 (1949).
[3] H. Sommer, H. A. Thomas, and J. A. Hipple, Phys. Rev. **82**, 697 (1951).
[4] *Ion Cyclotron Resonance Spectrometry*, edited by H. Hartmann and K.-P. Wanczek, Lecture Notes in Chemistry, Vol. 7 (Springer, Berlin, 1978).
[5] R. T. McIver, Jr., Rev. Sci. Instrum. **41**, 555 (1970).
[6] M. B. Comisarow and A. G. Marshall, Chem. Phys. Lett. **25**, 282 (1974).
[7] M. B. Comisarow and A. G. Marshall, J. Chem. Phys. **62**, 293 (1975).
[8] K.-P. Wanczek, Dyn. Mass Spectrom. **6**, 14 (1981).
[9] K.-P. Wanczek, Int. J. Mass Spectrom. Ion Proc. **60**, 11 (1984).
[10] K.-P. Wanczek, Int. J. Mass Spectrom. Ion Proc. **95**, 1 (1988).
[11] C. L. Johlman, R. L. White, and C. L. Wilkins, Mass Spectrom. Rev. **2**, 389 (1983).
[12] D. A. Laude, Jr., C. L. Johlman, R. S. Brown, D. A. Weil, and C. L. Wilkins, Mass Spectrom. Rev. **5**, 107 (1986).
[13] D. H. Russell, Mass Spectrom. Rev. **5**, 167 (1986).
[14] A. G. Marshall and F. R. Verdun, *Fourier Transforms in NMR, Optical, and Mass Spectrometry: A User's Handbook* (Elsevier, New York, 1990), p. 236.
[15] B. M. Smirnov, *Negative Ions* (McGraw-Hill, New York, 1982).
[16] M. R. Flannery, Chem. Phys. Lett. **80**, 541 (1981).
[17] C. J. Greaves, Electron. Control, **17**, 171 (1964).
[18] W. H. Aberth, J. R. Peterson, D. C. Lorents, and C. T. Cook, Phys. Rev. Lett. **20**, 979 (1968).
[19] J.-P. Schermann and F. G. Major, NASA Rep. X-524-71-343, Goddard Space Fight Center, Greenbelt, Maryland (1971).
[20] O. L. Rempel and M. L. Gross, Proceedings of the 39th American Conference on Mass Spectrometry and Allied Topics, Nashville (1991), p. 453.
[21] Y. Wang and K.-P. Wanczek, Proceedings of the 39th American Conference on Mass Spectrometry and Allied Topics, Nashville (1991), p. 1519.
[22] M. V. Gorshkov, S. Guan, and A. G. Marshall, Rapid Commun. Mass Spectrom. **6**, 166 (1992).
[23] J. L. Beauchamp, J. Chem. Phys. **46**, 1231 (1967).
[24] P. Kofel, M. Allemann, Hp. Kellerhals, and K.-P. Wanczek, Int. J. Mass Spectrom. Ion Phys. **46**, 139 (1983).
[25] R. C. Dunbar, J. H. Chen, and J. D. Hays, Int. J. Mass Spectrom. Ion Proc. **57**, 39 (1984).
[26] T. J. Francl, E. K. Fukuda, and R. T. McIver, Jr., Int. J. Mass Spectrom. Ion Phys. **50**, 151 (1983).
[27] J. B. Jeffries, S. E. Barlow, and G. H. Dunn, Int. J. Mass Spectrom. Ion Proc. **54**, 169 (1983).
[28] M. Wang and A. G. Marshall, Int. J. Mass Spectrom. Ion Proc. **100**, 323 (1990).
[29] M. B. Comisarow, J. Chem. Phys. **69**, 4097 (1978).
[30] A. Serreqi and M. B. Comisarow, Appl. Spectrosc. **41**, 288 (1987).
[31] D. A. Dahl and J. E. Delmore, SIMION PC/PS2, Version 4.0, Idaho National Engineering Laboratory (1988). Space Fight Center, Greenbelt, Maryland (1971).